

## Optical Properties and Electronic Structure of ZnSiAs<sub>2</sub>

J. L. Shay

*Bell Telephone Laboratories, Holmdel, New Jersey 07733*  
and

E. Buehler and J. H. Wernick

*Bell Telephone Laboratories, Murray Hill, New Jersey 07974*  
(Received 3 September 1970)

We report electroreflectance spectra for the chalcopyrite crystal ZnSiAs<sub>2</sub>. Structure in the electroreflectance spectra is observed at 2.12, 2.22, and 2.47 eV due to direct energy gaps in ZnSiAs<sub>2</sub> corresponding to the  $E_0$  and  $E_0 + \Delta_0$  direct energy gaps in zinc blende. The ordering and splittings of these transitions as well as their strong polarization dependences are explained quantitatively by a simple model which regards the chalcopyrite lattice as a compressed version of its binary analog. We also observe structure at 2.74 and 2.90 eV corresponding to the  $E_1$  and  $E_1 + \Delta_1$  structures in zinc blende. The splittings and polarization dependences agree with observations in stressed zinc-blende crystals. Much additional structure observed in ZnSiAs<sub>2</sub> is attributed to "pseudodirect" band gaps which result from the doubling of the unit cell in the  $Z$  direction in chalcopyrite relative to zinc blende. This change in the unit cell causes the Brillouin zone of zinc blende to be imbedded into the smaller Brillouin zone of chalcopyrite, and as a result new direct transitions can occur corresponding to indirect transitions in zinc blende. This is the first study of the electroreflectance spectra of a crystal which should have a pseudodirect transition as its lowest band gap. We do not observe this particular transition, and estimate that it is at least an order of magnitude weaker than the direct transitions derived from  $\Gamma_{15} \rightarrow \Gamma_1$  in zinc blende. We have also observed the dichroism of ZnSiAs<sub>2</sub> at a wavelength slightly below the lowest direct band gap. We find that the transmission is considerably higher for  $\vec{E} \perp Z$  than for  $\vec{E} \parallel Z$ , as predicted by the quasi-cubic model.

### I. INTRODUCTION

The II-IV-V<sub>2</sub> chalcopyrite semiconductors are of current interest from both experimental and theoretical points of view. Some of these crystals are potential candidates for visible-light semiconductor lasers, since they should have direct band gaps lying in the visible region of the spectrum and preliminary indications are that these crystals can be doped both  $n$  and  $p$  type.<sup>1</sup> Chalcopyrite crystals are uniaxial, and therefore they are birefringent. The magnitude of the birefringence in some ternaries is large enough to permit phase matching in nonlinear optical interactions.<sup>2</sup>

Theoretical interest in the chalcopyrites stems from the similarity of the chalcopyrite and zinc-blende lattices. One hopes that our understanding of the optical and electronic properties of zinc-blende crystals can be extrapolated to these ternaries. The pseudopotential method should be eminently applicable to this problem. Most band-structure calculations<sup>3</sup> have used perturbation theory<sup>4</sup> to extrapolate to chalcopyrite, but these calculations could not be critically evaluated, because of a lack of experimental data.

A simple theoretical model has recently been proposed<sup>5</sup> to explain the observed<sup>6</sup> splitting of the valence bands which result when the triple degeneracy of the  $\Gamma_{15}$  valence band in zinc blende is lifted in chalcopyrite. This model successfully explains

the ordering and splittings of the valence bands in CdSnP<sub>2</sub> and ZnSiAs<sub>2</sub> (the only crystals for which electroreflectance data are available) by regarding the chalcopyrite crystal as a strained version of its binary analog (e.g., InP is the binary analog of CdSnP<sub>2</sub>). It was further shown that a quasicubic model can be applied to chalcopyrite crystals, with the result that the polarization dependences for the three transitions derived from the  $\Gamma_{15} \rightarrow \Gamma_1$  transition in zinc blende are explained quantitatively.

In the present paper we present the electroreflectance spectra of single crystals of ZnSiAs<sub>2</sub>. We observe structure derived from the  $\Gamma_{15} \rightarrow \Gamma_1$  energy gap in zinc blende. The triple degeneracy of the  $\Gamma_{15}$  valence-band maximum in zinc blende is removed in chalcopyrite by the combined effects of the noncubic crystalline field and the spin-orbit interaction. As already mentioned, the ordering of these valence bands, as well as the polarization dependences of transitions to the conduction band, can be quantitatively explained by a simple model. We also observe structure corresponding to the  $E_1$  structures in zinc blende. The splitting and polarization dependences of these peaks agree with observations in stressed zinc-blende crystals.

In addition to these transitions corresponding to direct energy gaps in zinc blende, much additional structure is observed in ZnSiAs<sub>2</sub> due to pseudodirect band gaps which result from the doubling of the unit cell in chalcopyrite relative to zinc blende. This

change in the unit cell causes the Brillouin zone of zinc blende to be imbedded into the smaller Brillouin zone of chalcopyrite. Hence at every point in the chalcopyrite Brillouin zone, new direct transitions appear. We refer to these transitions as pseudodirect, since their strengths will depend upon the degree of difference of the pseudopotentials of the two cations.

Previous studies of the optical properties of  $\text{ZnSiAs}_2$  consist of photoconductivity<sup>7</sup> and absorption-coefficient<sup>8</sup> measurements which suggested that the band gap of  $\text{ZnSiAs}_2$  was 2.10 and  $2.16 \pm 0.03$  eV, respectively. Other workers reported the room-temperature energy gap to be 1.64<sup>9</sup> and 1.76<sup>10</sup> eV. From our electroreflectance data, we find that the lowest-energy gap in  $\text{ZnSiAs}_2$ , of the three derived from  $\Gamma_{15} \rightarrow \Gamma_1$  in zinc blende, lies at  $2.12 \pm 0.02$  eV, consistent with previous photoconductivity and absorption measurements. The nature of the previous measurements precluded a determination of the multiplicity of the valence band which results in chalcopyrite, or an observation of the pseudodirect band gaps which we report. A previous measurement<sup>11</sup> of the reflectivity of  $\text{ZnSiAs}_2$  found two broad maxima at 3.4 and 4.4 eV, respectively. In this same energy range we find six peaks in the electroreflectance spectra, most of which are strongly polarization dependent.

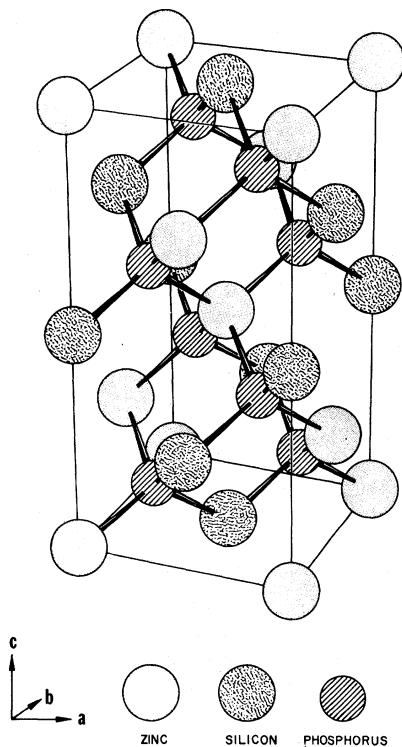


FIG. 1. Chalcopyrite unit cell [after S. C. A. Abrahams and J. L. Bernstein, *J. Chem. Phys.* **52**, 5607 (1970)].

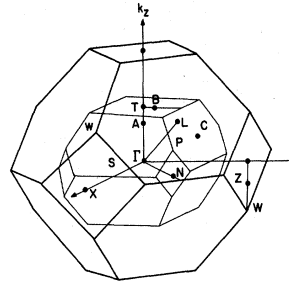


FIG. 2. Comparison of the Brillouin zones for chalcopyrite and zinc blende. The volume of the zinc-blende zone is four times that of the chalcopyrite zone.

## II. ENERGY-BAND STRUCTURE OF CHALCOPYRITE CRYSTALS

The similarity of the physical properties of zinc-blende III-V and chalcopyrite II-IV-V<sub>2</sub> crystals stems from the similarity of the crystal structures. The unit cell of the chalcopyrite lattice is shown in Fig. 1. Although the atomic positions in chalcopyrite are almost identical to those in zinc blende, there are three contributions to the non-cubic crystal potential: (a) The ordering of Zn and Si relative to one another is such that the unit cell is doubled along the Z axis; this contribution will be proportional to the differences in the pseudopotentials of the two cations; (b) the anions are not located at  $(\frac{1}{4}, \frac{1}{4}, \frac{1}{4})$ , etc., positions but are slightly distorted; and (c) the chalcopyrite lattice of  $\text{ZnSiAs}_2$  is slightly compressed along the Z axis.

The Brillouin zone for the chalcopyrite lattice is shown in Fig. 2 and compared with the zinc-blende Brillouin zone. The lowest-order approximation to the energy-band structure of a chalcopyrite crystal can be obtained merely by imbedding the band structure of its zinc-blende binary analog into the chalcopyrite Brillouin zone. A detailed discussion of this mapping has been given by Chaldyshev and Pokrovskii<sup>12</sup> and by Karavaev, Poplavnoi, and Chaldyshev.<sup>4</sup> Since the chalcopyrite zone is four times smaller than the zinc-blende zone, there are four times as many energy levels at every point in the chalcopyrite zone. Transitions between these levels are of two types: (i) direct transitions in chalcopyrite corresponding to direct transitions in zinc blende, and (ii) direct transitions in chalcopyrite corresponding to indirect transitions in zinc blende. We refer to these latter transitions as pseudodirect, since their strength will depend upon the differences of the cation pseudopotentials.

### Quasicubic Model

We first consider the triple degenerate  $\Gamma_{15} \rightarrow \Gamma_1$  transition which is split in chalcopyrite by the combined effects of the noncubic crystalline field and spin-orbit interaction. The valence-band model shown in Fig. 3 was originally proposed<sup>6</sup> to explain the polarization dependence observed in the  $\text{CdSnP}_2$

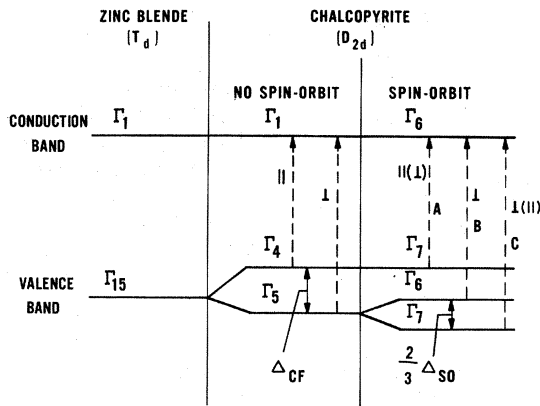


FIG. 3. Band structure and selection rules for the transitions in chalcopyrite derived from the  $\Gamma_{15} \rightarrow \Gamma_1$  energy gap in zinc blende. The splittings and polarization dependences are indicated schematically for a crystal in which  $\Delta_{so} \ll \Delta_{cf}$ . For arbitrary values of these parameters the valence-band splittings and polarization dependences are given, respectively, by Eqs. (1) and (3).

electroreflectance spectra. As shown in Fig. 3, in passing from zinc blende to chalcopyrite, the  $\Gamma_{15}$  valence band splits into a doubly degenerate  $\Gamma_5$  lying below the nondegenerate  $\Gamma_4$ . The polarization selection rules are as shown in the figure. With the inclusion of spin-orbit coupling,  $\Gamma_5$  splits into  $\Gamma_7$  and  $\Gamma_6$ , and the polarization selection rules are somewhat relaxed.

A simple theoretical model has been presented<sup>5</sup> which predicts quantitatively not only the ordering and splitting of the valence bands, but also the magnitude of the polarization dependences as well. This model regards the valence bands of a chalcopyrite crystal as equivalent to those of a strained version of its binary analog. Hopfield<sup>13</sup> has given the Hamiltonian matrix describing the splitting of the triple degenerate  $\Gamma_{15}$  valence band under the simultaneous perturbations of spin-orbit coupling and a uniaxial crystalline field. Within this so-called quasicubic model, the energies of the  $\Gamma_7$  levels relative to the  $\Gamma_6$  level in chalcopyrite are given by<sup>13,14</sup>

$$E_{1,2} = \frac{1}{2}(\Delta_{so} + \Delta_{cf}) \pm \frac{1}{2}[(\Delta_{so} + \Delta_{cf})^2 - \frac{8}{3}\Delta_{so}\Delta_{cf}]^{1/2}, \quad (1)$$

where  $\Delta_{so}$  is the spin-orbit splitting parameter and

$\Delta_{cf}$  is the crystal field splitting parameter. Considering only the effects of the compression of the chalcopyrite unit cell, we estimate  $\Delta_{cf}$  by

$$\Delta_{cf} = \frac{3}{2}b(2 - C/A), \quad (2)$$

where  $b$  is the deformation potential describing the splitting of the valence bands in the zinc-blende binary analog under uniaxial stress,<sup>15,16</sup> and  $C$  and  $A$  are the chalcopyrite lattice constants.<sup>17</sup> The spin-orbit parameter  $\Delta_{so}$  to be used in Eq. (1) is the average of the measured spin-orbit splitting  $\Delta_0$  in GaAs<sup>18</sup> and AlAs. Since  $\Delta_0$  has not been measured for AlAs, we have used the theoretical value of Herman *et al.*<sup>19</sup> The spin-orbit splitting and crystal field parameters predicted by this simple model are presented in Table I together with experimental values determined in a later section.

In addition to the eigenvalues given by Eq. (1), the quasicubic model determines eigenfunctions from which one can predict polarization dependences. For this model the ratio of the strengths of transitions from a given  $\Gamma_7$  valence band to the  $\Gamma_6$  conduction band for light polarized parallel or perpendicular, respectively, to the optic axis is given by<sup>13</sup>

$$I_{||}/I_{\perp} = (2 - 3E/\Delta_{so})^2. \quad (3)$$

Using experimental values for  $E$  and  $\Delta_{so}$ , the predictions of Eq. (3) for ZnSiAs<sub>2</sub> are given in Table I together with experimental intensity ratios determined in a later section. The intensity ratio predicted by Eq. (3) is also shown as the solid line in

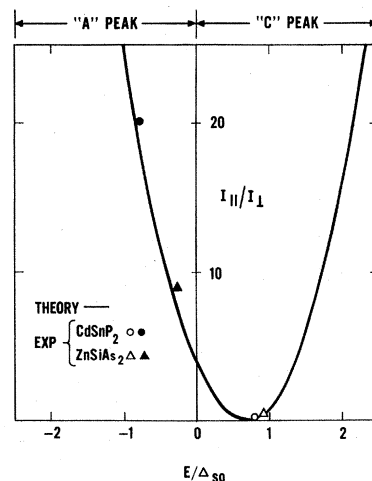


FIG. 4. Ratio of the strengths of transitions from a given  $\Gamma_7$  valence band to the  $\Gamma_6$  conduction band for light polarized parallel or perpendicular, respectively, to the optic axis. The solid line is the theoretical result of the quasicubic model from Eq. (3). The experimental points are taken from A ( $\bullet$ ,  $\blacktriangle$ ) and C ( $\circ$ ,  $\blacktriangle$ ) peaks of electroreflectance data.  $E$  is the energy of a  $\Gamma_7$  valence-band state relative to the  $\Gamma_6$  valence band, and  $\Delta_{so}$  is the spin-orbit-splitting parameter.

TABLE I. Comparison of experimental results and theoretical predictions of the quasicubic model for the valence-band structure of ZnSiAs<sub>2</sub>.

	$\Delta_{so}$ (eV)	$\Delta_{cf}$ (eV)	A	$I_{  }/I_{\perp}$	
				B	C
Experiment	0.28	-0.13	9	~0	~0.5
Theory	0.31	-0.16	8.5	0	0.5

Fig. 4, where the points are experimental data for  $\text{CdSnP}_2$ <sup>6</sup> and the present results for  $\text{ZnSiAs}_2$ . The quasicubic model quantitatively explains the observed polarization dependences.

#### $E_1$ and $E_1 + \Delta_1$ Energy Gaps

A quasicubic model can also be constructed for the spin-orbit-split  $E_1$  and  $E_1 + \Delta_1$  energy gaps which occur in the  $\Delta$  direction in zinc blende. Although the  $L$  point in zinc blende maps to  $N$  in chalcopyrite (see below), most of the  $\Delta$  direction is preserved. Consequently, if the  $E_1$  transitions occur close enough to  $\mathbf{k} = (0, 0, 0)$  in zinc blende, they should also appear in chalcopyrite. No estimates are available for chalcopyrite crystals, but for Ge and GaAs it is believed<sup>15</sup> that these transitions are centered  $\sim 40\%$  of the distance to  $L$  from  $\Gamma$  and should therefore be preserved in chalcopyrite.

Uniaxial strain of a zinc-blende crystal<sup>15</sup> increases the splitting of the  $E_1$  peaks, and causes the amplitudes to depend upon the polarization of the incident radiation. In a chalcopyrite crystal, the splitting of the  $E_1$  peaks can therefore be approximated by

$$\Delta_1^{\text{ch}} = [(\Delta_1)^2 + (\frac{1}{3}\Delta_{\text{cf}})^2]^{1/2}, \quad (4)$$

where  $\Delta_{\text{cf}}$  is the crystal field parameter given by Eq. (2). The compression of the chalcopyrite lattice causes the intensity of the  $E_1$  peaks to become polarization dependent<sup>15</sup> to an extent which depends upon the parameter  $\alpha_1 \equiv -\frac{1}{3}(\Delta_{\text{cf}}/\Delta_1)$ :

$$E_1 : \frac{I_{\parallel}}{I_{\perp}} = \frac{1 + \alpha_1}{1 - \frac{1}{2}\alpha_1},$$

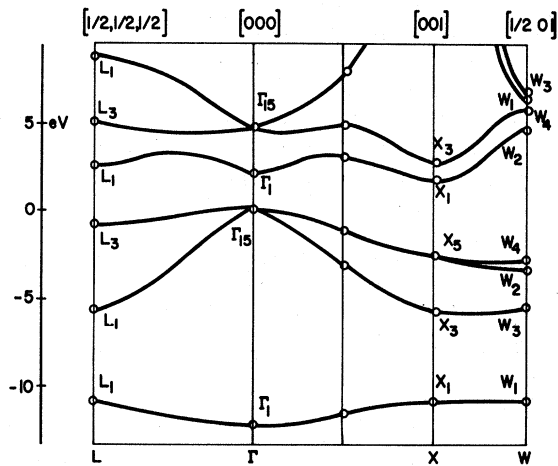


FIG. 5. Energy-band structure calculated by Poplavnoi (Ref. 3) for a hypothetical zinc-blende modification of  $\text{ZnSiAs}_2$ . The cation pseudopotential was set equal to the average of the pseudopotentials of Zn and Si, and the pseudopotential of As was placed at the anion sites.

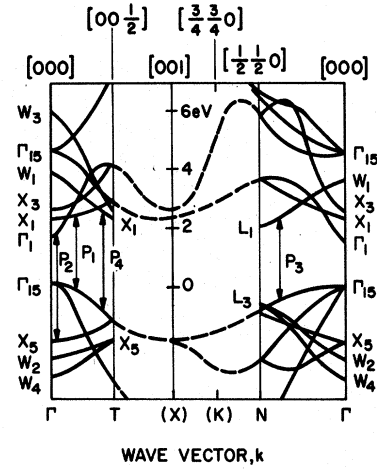


FIG. 6. Energy-band structure of  $\text{CdSnP}_2$  (solid lines) obtained by imbedding the band structure of InP (dashed lines) into the chalcopyrite Brillouin zone. The information in Fig. 5 is not sufficient to allow such a figure to be constructed for  $\text{ZnSiAs}_2$ . Our purpose here is to show schematically the locations in the Brillouin zone of the pseudodirect transitions  $P_1$ - $P_4$  which are derived from indirect transitions in zinc blende.

$$E_1 + \Delta_1 : \frac{I_{\parallel}}{I_{\perp}} = \frac{1 - \alpha_1}{1 + \frac{1}{2}\alpha_1}. \quad (5)$$

Equations (4) and (5) give a satisfactory account of the  $E_1$  peaks observed in the electroreflectance spectra of  $\text{CdSnP}_2$ <sup>6,20</sup> and the  $\text{ZnSiAs}_2$  spectra given in a later section.

#### Pseudodirect Energy Gaps

The energy-band structure calculated by Poplavnoi<sup>3</sup> for  $\text{ZnSiAs}_2$  in a hypothetical zinc-blende structure is shown in Fig. 5. For this calculation, the average of the pseudopotentials of Zn and Si was placed at each cation site in the zinc-blende lattice. An approximation to the band structure of  $\text{ZnSiAs}_2$  in the chalcopyrite lattice can be obtained merely by imbedding the band structure shown in Fig. 5 into the chalcopyrite Brillouin zone<sup>4,12</sup> (Fig. 2). Since the energy bands at  $W$  and along the  $\Sigma$  direction in  $\text{ZnSiAs}_2$  were not reported by Poplavnoi,<sup>3</sup> the result of this mapping is shown in Fig. 6 for some of the high-symmetry directions in  $\text{CdSnP}_2$ . The points  $X$  and  $W$  in zinc blende both map to  $\Gamma$  in chalcopyrite and  $L$  maps to  $N$ . As a result of this reduction in the size of the Brillouin zone, at each point there appear several new direct transitions corresponding to indirect transitions in zinc blende. Since the strength of these transitions depends upon the degree of difference of the pseudopotentials of the two cations, we refer to these new transitions as "pseudodirect."

Typical pseudodirect transitions are labeled

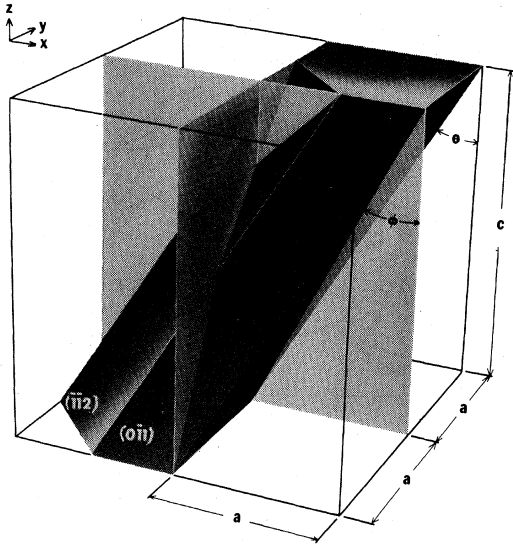


FIG. 7. Habit of growth of  $\text{ZnSiAs}_2$  crystals (after Ref. 22).

$P_1$ – $P_4$  in Fig. 6, although clearly there are many other possibilities. The polarization dependence of these transitions can be determined from published character tables.<sup>12,14</sup>  $P_1$  and  $P_2$  are expected to be observed principally for  $\vec{E} \perp Z$ , although spin-orbit interaction will relax this restriction somewhat.  $P_3$  should be observed for both polarizations, and  $P_4$  should be strongly polarized  $\vec{E} \parallel Z$ .

### III. EXPERIMENTAL TECHNIQUES

The  $\text{ZnSiAs}_2$  crystals were grown by a closed-tube chemical-transport technique using a small amount ( $\sim 0.3\%$  by weight of the total charge) of  $\text{SnCl}_2$  as the source of  $\text{Cl}_2$  for the transport of Si. They were irregular in shape but showed several facets about  $3 \times 6$  mm in size. Although not intentionally doped, the crystals were  $p$  type with a resistivity of about  $10 \Omega \text{ cm}$ . A more detailed discussion of the crystal growth will be presented elsewhere.<sup>21</sup>

The habit of growth for chalcopyrite crystals<sup>22</sup> is shown in Fig. 7. The identification of the major facets was confirmed by Laue photographs and x-ray diffraction studies. For reflectance studies on (112) and (011) faces, it is possible to polarize light with the electric vector perpendicular to the optic axis, but not completely parallel to this axis. Consequently in the electroreflectance spectra,  $\vec{E} \parallel Z$  is only nominal, and in fact only  $\frac{2}{5}$  or  $\frac{4}{5}$  of the intensity lies parallel to  $Z$  for (112) and (011) faces, respectively.

The electroreflectance measurements were performed using the electrolyte technique developed by Cardona and co-workers.<sup>18</sup> Identical spectra were obtained from natural surfaces that were

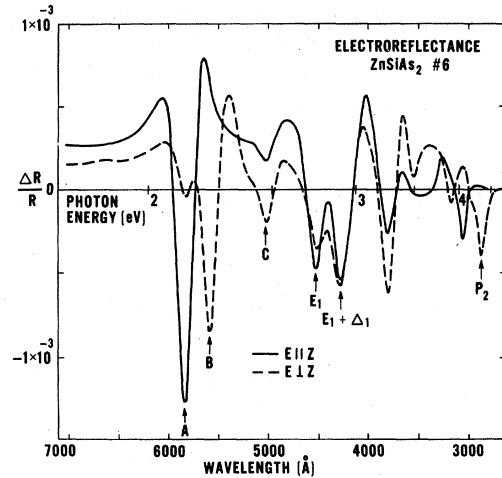


FIG. 8. Electrolyte electroreflectance spectra of  $\text{ZnSiAs}_2$  for light polarized relative to the optic axis. The orientation was nearly (011), so  $\vec{E} \parallel Z$  is only nominal and only  $\frac{4}{5}$  of the intensity is parallel to  $Z$ .  $V_{dc} = -1.5 \text{ V}$ ;  $V_{ac} = 1.0 \text{ V}_{pp}$ .

Syton<sup>23</sup> polished or etched in a 5% bromine methanol solution for 2 min. Soldered indium contacts made Ohmic contact to the crystals.

### IV. EXPERIMENTAL RESULTS

In Fig. 8 we present electroreflectance spectra for a single crystal of  $\text{ZnSiAs}_2$  measured, respectively, for light polarized parallel and perpendicular to the optic axis. The offset at long wavelengths varied considerably from one crystal to another and probably is due to free carriers. The offset is not due to the electrolyte, since it was also present in unpublished photorefectance spectra. Since we have no way of knowing how far up in energy the offset goes, the data may be somewhat distorted. The general features of the data in Fig. 8 agree with the unpolarized data of Kwan and Woolley<sup>24</sup> obtained on polycrystalline samples, although their interpretation is considerably different from ours. The

TABLE II.  $\text{ZnSiAs}_2$  electroreflectance structure.

Label	Energy (eV)	Polarization	Identification	Zinc-blende analog
A	2.12	$\parallel, \perp$	$\Gamma_7 \rightarrow \Gamma_6$	$E_0$ $E_0 + \Delta_0$
B	2.22	$\perp$	$\Gamma_6 \rightarrow \Gamma_6$	
C	2.47	$\perp, \parallel$	$\Gamma_7 \rightarrow \Gamma_6$	
$E_1$	2.74	$\parallel, \perp$	$\Lambda_3 \rightarrow \Lambda_1$	$E_1$
$E_1 + \Delta_1$	2.90	$\perp, \parallel$	$\Lambda_3 \rightarrow \Lambda_1$	$E_1 + \Delta_1$
	3.25	$\perp, \parallel$		
	3.91	$\perp$		
	4.04	$\parallel$		
$P_2$	4.31	$\perp$	$X_5 \rightarrow \Gamma_1$	

energies of all peaks, their polarization properties, and our assignments are summarized in Table II.

The  $A$ ,  $B$ , and  $C$  transitions at 2.12, 2.22, and 2.47 eV in Fig. 8 are derived from the  $\Gamma_{15} \rightarrow \Gamma_1$  transition in zinc blende according to the model shown in Fig. 3 due to the simultaneous perturbations of spin-orbit interaction and the noncubic crystalline field. The parameters of the model  $\Delta_{cf}$  and  $\Delta_{so}$  as determined from experimental data using Eq. (1) are given in Table I, together with the theoretical predictions determined earlier. It is to be expected that our theoretical model based on compression alone should slightly overestimate the negative crystal field splitting, since calculations<sup>3</sup> for similar chalcopyrite crystals have shown that the first two noncubic potentials listed earlier produce a small positive  $\Delta_{cf}$  which would tend to improve the already good agreement between theory and experiment in Table I.

The quasicubic model is also able to quantitatively explain the magnitude of the polarization dependences of the  $A$ ,  $B$ , and  $C$  peaks observed in Fig. 8. Using the experimental values for  $\Delta_{so}$  and  $\Delta_{cf}$ , the theoretical intensity ratios calculated using Eq. (3) are listed in Table I and compared with the experimental data taken from Fig. 8. These data are also shown in Fig. 4 together with published data for  $\text{CdSnP}_2$ ,<sup>6,20</sup> and compared with the theoretical prediction of Eq. (3). The quasicubic model quantitatively explains the observed polarization dependences.

The two transitions at 2.74 and 2.90 eV in Fig. 8 are assigned to the same transitions that produce the  $E_1$  and  $E_1 + \Delta_1$  peaks in zinc blende. The basis for this identification is that the splitting of these peaks is very nearly  $\frac{2}{3}$  of the spin-orbit splitting of the  $\Gamma_{15} \rightarrow \Gamma_1$  transitions (Table I). This so-called " $\frac{2}{3}$  rule" is usually obeyed in all zinc-blende crystals.<sup>18</sup> Actually, the splitting of the  $E_1$  peaks should be somewhat larger in chalcopyrite because of the compression of the lattice along the  $Z$  axis. According to Eq. (4),  $\Delta_1^{\text{ch}} = 0.19$  eV, which is in reasonable agreement with the measured splitting of 0.16 eV. Further evidence supporting our identifications of the  $E_1$  and  $E_1 + \Delta_1$  transitions in  $\text{ZnSiAs}_2$  is that the polarization dependence of these peaks agrees with observations in stressed zinc-blende crystals. For  $\text{ZnSiAs}_2$ ,  $\alpha_1 = 0.24$  and Eq. (5) predicts that  $I_{\parallel}/I_{\perp} = 1.41$  and 0.68 for the  $E_1$  and  $E_1 + \Delta_1$  peaks, respectively. The agreement with theory is good for the  $E_1$  peak but not for the  $E_1 + \Delta_1$  peak. Nonetheless, the polarization dependences of the  $E_1$  peaks are smaller in  $\text{ZnSiAs}_2$  than in  $\text{CdSnP}_2$  as the trend in  $\alpha_1$  predicts. Kesamanly *et al.*<sup>11</sup> observed a broad reflection peak in  $\text{ZnSiAs}_2$  near 3.4 eV, about 0.5 eV wide, which they identified as the  $E_1$  and  $E_1 + \Delta_1$  transitions although the splitting was not resolved. This interpretation is not consistent

with our results, which locate the  $E_1$  and  $E_1 + \Delta_1$  transitions at 2.74 and 2.90 eV (Fig. 8).

Poplavnoi's<sup>3</sup> pseudopotential calculation indicates that these peaks should lie near 3.5 eV, about 0.7 eV above our experimental result. The explanation for this discrepancy between theory and experiment in  $\text{ZnSiAs}_2$  (and a similar discrepancy in  $\text{CdSnP}_2$ <sup>20</sup>) is not understood. Kwan and Woolley<sup>24</sup> find a similar shift ( $\sim 0.4$  eV) as they follow the  $E_1$  and  $E_1 + \Delta_1$  peaks through the  $\text{InAs-CdSnAs}_2$  alloy system.

The four remaining structures at 3.25, 3.91, 4.04, and 4.31 eV in Fig. 8 are attributed to pseudodirect transitions, since they occur in an energy range between the  $E_1$  transitions and the higher-energy  $E'_0$  and  $E_2$  transitions in the hypothetical binary analog  $\frac{1}{2}(\text{GaAs and AlAs})$ . As discussed earlier, these pseudodirect transitions are direct transitions in chalcopyrite corresponding to indirect transitions in zinc blende, and occur due to the mapping of the zinc-blende Brillouin zone into the smaller chalcopyrite Brillouin zone. Typical pseudodirect transitions  $P_1 - P_4$  are shown in Fig. 6. Since  $X_1$  lies below  $\Gamma_1$  in Fig. 5, the pseudodirect transition  $P_1$  is expected to be the lowest-energy direct transition in  $\text{ZnSiAs}_2$ , lying  $\sim 0.2$  eV below the  $A$  transition in the electroreflectance spectrum. It can be seen in Fig. 8, however, that there is no strong structure in this region, only a weak bump at 1.9 eV for  $\vec{E} \perp Z$ . Although  $P_1$  is expected to be strongly polarized  $\vec{E} \perp Z$ , the structure is not very reproducible from one sample to another and may be due to impurities. We conclude that this pseudodirect transition is at least an order of magnitude weaker than the  $A$ ,  $B$ , and  $C$  direct transitions.

The assignment of a electroreflectance structure to a specific pseudodirect transition is based on the observed polarization dependence, and the energy of the equivalent (forbidden) transition in the zinc-blende binary analog. Although electroreflectance structure due to  $P_2$ ,  $P_3$ , and  $P_4$  was observed in  $\text{CdSnP}_2$ ,<sup>6,20</sup> only the  $P_2$  transition is identified in the present data for  $\text{ZnSiAs}_2$ . Estimating the energy of  $X_5$  from its value in  $\text{GaAs}$ <sup>25</sup> and  $\text{AlAs}$ <sup>26</sup> or from the band structure in Fig. 5,  $P_2$  should lie near 4.3 eV. Experimentally we find a peak lying at 4.31 eV and strongly polarized  $\vec{E} \perp Z$ , which we therefore assign to the pseudodirect transition  $P_2$ . The assignment of the remaining structure in Fig. 8 must await a more complete energy-band calculation for chalcopyrite crystals.

The band-structure model in Fig. 3 predicts that the absorption edge shown in Fig. 9 should be dichroic. To investigate this effect, we have measured the transmission of a platelet of  $\text{ZnSiAs}_2$  as the platelet is rotated about the direction of propagation of a He-Ne laser at 6328 Å (1.96 eV). The

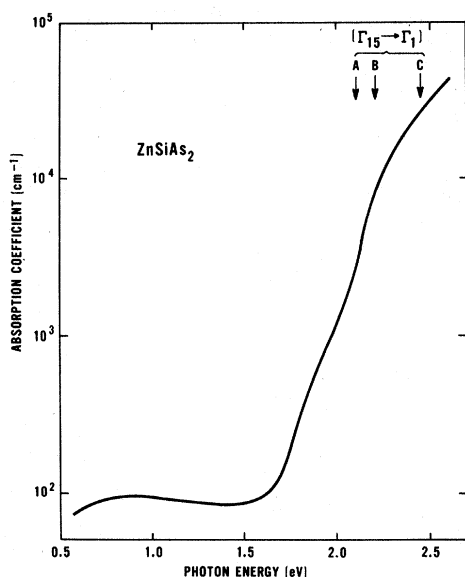


FIG. 9. Absorption coefficient of  $\text{ZnSiAs}_2$  after Ref. 8. The arrows labeled A, B, and C indicate the direct transitions observed in the electroreflectance spectra (Fig. 8) and derived from the  $\Gamma_{15} \rightarrow \Gamma_1$  transition in zinc blende.

results of this experiment are shown in Fig. 10, where the data have been fitted to an equation of the form

$$T(\theta) = T_x \cos^2(\theta) + T_y \sin^2(\theta). \quad (6)$$

Since the natural face was nearly (011),  $\vec{E} \parallel Z$  is only nominal as explained earlier. In agreement with the model in Fig. 3, we find that the transmission is considerably higher for  $\vec{E} \perp Z$  than for  $\vec{E} \parallel Z$ .

## V. CONCLUSIONS

In summary, we have shown that the electroreflectance structure near the lowest direct band gap of  $\text{ZnSiAs}_2$  is derived from the  $\Gamma_{15} \rightarrow \Gamma_1$  direct gap of zinc blende, but is split by the combined effects of the noncubic crystalline field and spin-orbit interaction. We have shown that the signs and magnitudes of these splittings can be predicted by the quasicubic model, taking into account only spin-orbit coupling and the uniaxial compression of the chalcopyrite lattice. The strong polarization dependences of these band-edge transitions as observed in the electroreflectance spectra are also explained quantitatively by the quasicubic model. We have also observed structure in the electro-

reflectance spectra due to states derived from the  $E_1$  and  $E_1 + \Delta_1$  band gaps in zinc blende. The splitting of these peaks and the polarization dependences are consistent with electroreflectance studies of stressed cubic semiconductors.

In addition to this electroreflectance structure due to direct band gaps in  $\text{ZnSiAs}_2$  derived from direct band gaps in zinc blende, we observe much additional structure due to pseudodirect transitions — direct transitions in chalcopyrite derived from indirect transitions in zinc blende. These pseudodirect gaps result when many points in the zinc-blende Brillouin zone are mapped into any one point in the chalcopyrite Brillouin zone due to the doubling of the unit cell along the optic axis in chalcopyrite. We have identified the origins of some of this structure from the observed polarization dependences and from a knowledge of the energies of the equivalent (forbidden) transitions in zinc blende. Some remaining structure has not been identified and we anxiously await a more complete energy-band calculation for chalcopyrite crystals.

## ACKNOWLEDGMENTS

We thank Professor J. C. Woolley for sending us a report of his work prior to publication, C. K. N. Patel for critically reading the manuscript, and J. E. Rowe for his collaboration in the portion of this work reported in Ref. 5. We also thank L. M. Schiavone for technical assistance, and Mrs. A. A. Pritchard for crystal polishing and other technical assistance.

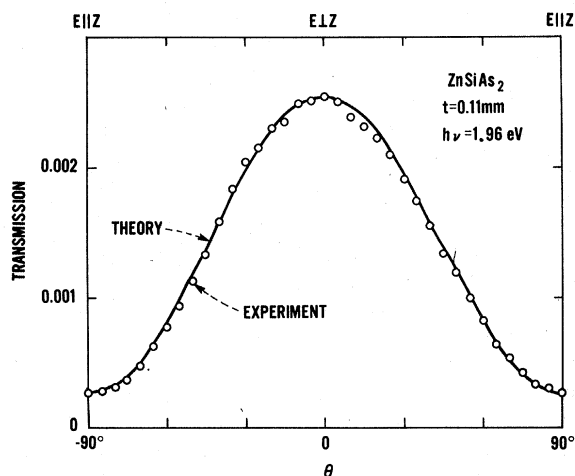


FIG. 10. Transmission of a He-Ne laser ( $6328 \text{ \AA}$ ) through a platelet of  $\text{ZnSiAs}_2$  as the polarization is varied. Since the orientation is nearly (011),  $\vec{E} \parallel Z$  is only nominal, and only  $\frac{4}{5}$  of the intensity is along Z.

<sup>1</sup>For a recent review, see N. A. Goryunova, in *Proceedings of the Ninth International Conference on the Physics of Semiconductors*, edited by S. M. Ryvkin (Nauka, Leningrad, 1968), p. 1198.

<sup>2</sup>G. D. Boyd (private communication).

<sup>3</sup>ZnSnP<sub>2</sub>: N. A. Goryunova, M. L. Belle, L. B. Llatkin, G. V. Loskova, A. S. Poplavnoi, and V. A. Chaldyshev, *Fiz. Tekh. Popuprov.* **2**, 1344 (1968) [*Soviet Phys. Semicond.* **2**, 1126 (1969)]; ZnGeAs<sub>2</sub> and ZnSiP<sub>2</sub>: A. S. Poplavnoi and G. F. Karavaev, *Izv. Akad. Nauk SSSR Neorgan. Materialy* **4**, 196 (1968); ZnSnAs<sub>2</sub>: A. S. Poplavnoi, *Izv. Akad. Nauk SSSR Neorgan. Materialy* **5**, 498 (1969) [*Bull. Acad. Sci. USSR Ser. Inorg. Mater.* **5**, 415 (1969)]; ZnSiAs<sub>2</sub> and ZnGeP<sub>2</sub>: A. S. Poplavnoi, *Izv. Viz. Fiz. SSSR* **11**, 142 (1968); nonperturbative, MgSiP<sub>2</sub>, ZnSiP<sub>2</sub>, ZnGeP<sub>2</sub>, ZnSiAs<sub>2</sub>, CdSiP<sub>2</sub>, ZnSnP<sub>2</sub>, CdSnP<sub>2</sub>, ZnGeAs<sub>2</sub>, CdGeAs<sub>2</sub>, ZnSnAs<sub>2</sub>, CdGeP<sub>2</sub>, and CdSiAs<sub>2</sub>: N. A. Goryunova, A. S. Poplavnoi, Yu. I. Polygalov, and V. A. Chaldyshev, *Phys. Status Solidi* **39**, 9 (1970).

<sup>4</sup>G. F. Karavaev and A. S. Poplavnoi, *Fiz. Tverd. Tela* **8**, 2143 (1966) [*Soviet Phys. Solid State* **8**, 1704 (1967)]; G. F. Karavaev, A. S. Poplavnoi, and V. A. Chaldyshev, *Fiz. Tekh. Poluprov.* **2**, 113 (1968) [*Soviet Phys. Semicond.* **2**, 93 (1968)].

<sup>5</sup>J. E. Rowe and J. L. Shay, *Phys. Rev. B* (to be published).

<sup>6</sup>J. L. Shay, E. Buehler, and J. H. Wernick, *Phys. Rev. Letters* **24**, 1301 (1970); J. L. Shay, E. Buehler, and J. H. Wernick, in *Proceedings of the Tenth International Conference on the Physics of Semiconductors*, edited by S. P. Keller, J. C. Hensel, and F. Stern (U. S. Atomic Energy Commission, 1970), p. 589.

<sup>7</sup>F. P. Kesamanly, Yu. V. Rud', and S. V. Slobodchikov, *Dokl. Akad. Nauk SSSR* **161**, 1065 (1965) [*Soviet Phys. Doklady* **10**, 336 (1965)].

<sup>8</sup>J. E. Snell, G. J. Burrell, T. S. Moss, and J. C. Maberly, in *Proceedings of the Ninth International Conference on the Physics of Semiconductors*, edited by S. M. Ryvkin (Nauka, Leningrad, 1968), p. 1227.

<sup>9</sup>A. A. Vaipolin, N. A. Goryunova, E. O. Osmanov, Yu. V. Rud', and D. N. Tret'yakov, *Dokl. Akad. Nauk SSSR* **154**, 1116 (1964).

<sup>10</sup>A. A. Vaipolin, F. M. Gashimzade, N. A. Goryunova, F. P. Kesamanly, D. N. Nasledov, E. O. Osmanov, and Yu. V. Rud', *Izv. Akad. Nauk SSSR Ser. Fiz.* **28**,

1085 (1964) [*Bull. Acad. Sci. USSR Phys. Ser.* **28**, 984 (1965)].

<sup>11</sup>F. P. Kesamanly, S. G. Kroitoru, Yu. V. Rud', V. V. Sobolev, and N. N. Syrbu, *Dokl. Akad. Nauk SSSR* **163**, 868 (1965) [*Soviet Phys. Doklady* **10**, 743 (1966)].

<sup>12</sup>V. A. Chaldyshev and V. N. Pokrovskii, *Izv. Viz. Fiz. SSSR* **2**, 173 (1960); **5**, 103 (1963).

<sup>13</sup>J. J. Hopfield, *J. Phys. Chem. Solids* **15**, 97 (1960). Our sign conventions for Eqs. (1) and (3) are in agreement with this reference.

<sup>14</sup>Our symmetry notation is taken from G. F. Koster, J. O. Dimmock, R. G. Wheeler, and H. Statz, *Properties of the Thirty-Two Point Groups* (MIT Press, Cambridge, Mass., 1963). A single exception is the zinc blende level  $\Gamma_{15}$ , which we identify with  $\Gamma_5$  in the point group  $T_d$ . In the Russian literature a quite different notation is used for the extra representations of the chalcopyrite point group  $D_{2d}$ .

<sup>15</sup>F. H. Pollak and M. Cardona, *Phys. Rev.* **172**, 816 (1968).

<sup>16</sup>A. Gavini and M. Cardona, *Phys. Rev. B* **1**, 672 (1970).

<sup>17</sup>A. S. Borshevskii, N. A. Goryunova, F. T. Kesamanly, and D. N. Nasledov, *Phys. Status Solidi* **21**, 9 (1967).

<sup>18</sup>M. Cardona, K. L. Shaklee, and F. H. Pollak, *Phys. Rev.* **154**, 696 (1967); M. Cardona, in *Solid State Physics*, edited by F. Seitz and D. Turnbull (Academic, New York, 1969), Suppl. 11.

<sup>19</sup>F. Herman, C. D. Kuglin, K. F. Cuff, and R. L. Kortum, *Phys. Rev. Letters* **11**, 541 (1963).

<sup>20</sup>J. L. Shay, E. Buehler, and J. H. Wernick, *Phys. Rev. B* **2**, 4104 (1970).

<sup>21</sup>E. Buehler and J. H. Wernick, *J. Crystal Growth* (to be published).

<sup>22</sup>I. P. Kaminow, E. Buehler, and J. W. Wernick, *Phys. Rev. B* **2**, 960 (1970).

<sup>23</sup>Syton HT, Monsanto Chemical Co., 277 Park Ave., New York, N. Y. 10017.

<sup>24</sup>C. C. Y. Kwan and J. C. Woolley, *Can. J. Phys.* **48**, 2085 (1970).

<sup>25</sup>M. L. Cohen and T. K. Bergstresser, *Phys. Rev.* **141**, 789 (1966); J. A. Van Vechten, *ibid.* **187**, 1007 (1969).

<sup>26</sup>D. J. Stukel and R. N. Euwema, *Phys. Rev.* **188**, 1193 (1969).



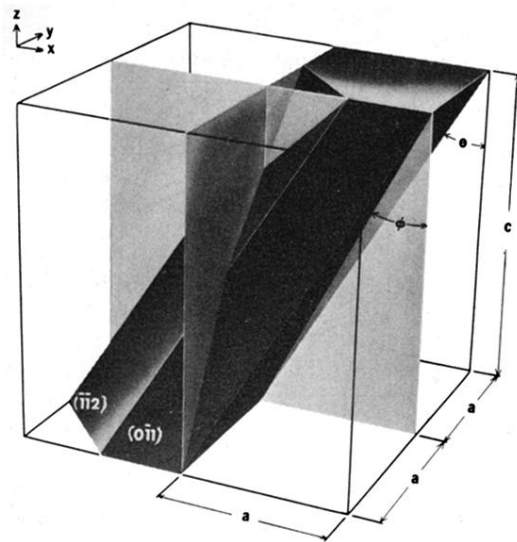


FIG. 7. Habit of growth of ZnSiAs<sub>2</sub> crystals (after Ref. 22).